Energy cascades in active-grid-generated turbulent flows

D. O. Mora,* E. Muñiz Pladellorens, P. Riera Turró, M. Lagauzere, and M. Obligado†
Université Grenoble Alpes, CNRS, Grenoble INP, LEGI, 38000 Grenoble, France

(Received 6 May 2019; published 4 October 2019)

The energy cascade and diverse turbulence properties of active-grid-generated turbulence were studied in a wind tunnel via hot-wire anemometry. To this end, two active grid protocols were considered. The first protocol is the standard triple-random mode, where the grid motors are driven with random rotation rates and directions, which are changed randomly in time. This protocol has been extensively used due to its capacity to produce higher values of Re_λ than its passive counterpart, with good statistical homogeneity and isotropy. The second protocol was a static or open grid mode, where all grid blades were completely open, yielding the minimum blockage attainable with our grid. Center-line streamwise profiles were measured for both protocols and several inlet velocities. It was found that the turbulent flow generated with the triple-random protocol evolved in the streamwise direction consistently with an energy dissipation scaling of the form $\varepsilon = C_\varepsilon u'^3/L$, with C_ε being a constant, L the longitudinal integral length scale, and u' the rms of the longitudinal velocity fluctuations. Conversely, for the open-static grid mode, the energy dissipation followed a nonequilibrium turbulence scaling, namely, $C_\varepsilon \sim \mathrm{Re}_G/\mathrm{Re}_L$, where Re_G is a global Reynolds number based on the inlet conditions of the flow and Re_L is based on the local properties of the flow downstream the grid. Furthermore, this open-static grid mode scaling exhibits important differences with other grids, as the downstream location of the peak of turbulence intensity is a function of the inlet velocity; a remarkable observation that would allow one to study the underlying principles of the transition between equilibrium and nonequilibrium scalings, which are yet to be understood. It was also found that a rather simple theoretical model can predict the value of C_ε based on the number density of zero crossings of the longitudinal velocity fluctuations. This theory is valid for both active grid operating protocols (and therefore two different energy cascades).

DOI: 10.1103/PhysRevFluids.4.104601

I. INTRODUCTION

Since the first active grid was proposed by Makita [1], active-grid-generated turbulence has become a standard way to generate moderate-to-high Reynolds numbers in wind/water tunnels [2]. They present several advantages over classical passive grids for wind/water tunnel research, as bespoke nonstationary or inhomogeneous turbulence with relatively large values of Reynolds numbers based on the Taylor microscale, Re_λ, and reasonable homogeneous isotropic turbulence (HIT) conditions, can be generated with active grids. Their use has therefore become widespread in several active research fields, such as two-phase [3,4] and atmospheric flows [5], wind energy [6], and fundamental turbulence [7–10].

In many of these applications, these grids are used to "tune" the turbulence intensity and/or the Reynolds number Re_λ. Several grid protocols are then available to explore the parameter space,

*Department of Mechanical Engineering, University of Washington, Seattle, Washington 98195-2600, USA.
†martin.obligado@univ-grenoble-alpes.fr

but little or no attention has been paid yet to the consequences of them on the energy cascade. For instance, some studies have focused on the characteristics of the turbulent flow for a given blade geometry and initial conditions [11]. Furthermore, other studies have reported values of the turbulent kinetic energy dissipation constant C_ε [12,13], primarily by employing one operating protocol with subtle variations (the one defined as triple random below), with the intent to corroborate the validity of the scalings derived from Kolmogorov's 1941 theory (K41), also detailed below. C_ε is a key parameter to understand these flows, as it can be used to determine the properties of the energy cascade on them (for further details, we refer to the review from Vassilicos [14]).

Therefore, it remains unclear whether the nature of the energy cascade would remain unchanged if strong changes were to be introduced in the grid controlling protocol. The traditional view, derived from Kolmogorov's scalings (and compatible with both of his 1941 and 1962 theories), is that the turbulent kinetic energy dissipation follows the law $\varepsilon = C_\varepsilon \frac{u'^3}{L}$, where u' is the standard deviation of streamwise velocity fluctuations u and L is the longitudinal integral length scale. C_ε is a constant that may depend on the boundary conditions but remains constant for a fixed grid geometry. Recently, several separate studies have reported that these scalings may also be fulfilled within a balanced non-equilibrium cascade [15]. From now on, we will refer to these scalings as "standard" dissipation scalings.

It has been known for some time that grids can generate a region where turbulence is at odds with these laws, i.e., C_ε is not constant, but instead it goes as $C_\varepsilon \sim \mathrm{Re}_G^m/\mathrm{Re}_L^n$, where Re_G is a Reynolds number that depends on the inlet conditions and Re_L is a local, streamwise position-dependent one [14]. The exponents n and m have been found to be very close to unity; $m = n = 1$ for large values of Re_λ. For grid turbulence, $\mathrm{Re}_G = MU_\infty/\nu$, with M being the mesh spacing, U_∞ the inlet velocity, and ν the kinematic viscosity of the flow. The local Reynolds number is defined as $\mathrm{Re}_L = Lu'/\nu$. These high Reynolds nonequilibrium scalings have been recovered in both regular and fractal grids, at a range of downstream positions which starts close to the peak of turbulent kinetic energy and extends well beyond it. Typically, this region spans $x_{\max} < x < 5x_{\max}$, where x is the downstream coordinate from the grid and $x_{\max}$ (see details below) can be predicted as the position where the wakes of the grid bars meet, which hinges on the grid geometry.

The presence of diverse energy cascades would create limitations for the applicability of active grids in some situations, as their respective consequences regarding scales separation, and the number of degrees of freedom (quantified by L/λ), would follow separate laws. "Standard" scalings verify the relation $L/\lambda \sim C_\varepsilon \mathrm{Re}_\lambda$, while high Reynolds nonequilibrium scalings preserve $L/\lambda \sim \sqrt{\mathrm{Re}_G}$ (where both formulas assume $\varepsilon \sim \nu u'^2/\lambda^2$). The latter are independent of Re_λ at fixed Re_G.

This work summarizes a series of experiments on active-grid-generated turbulence. We found evidence that different operating protocols produce different energy cascades. Given the myriad of possible operating protocols, we focused on two extreme cases: one where the grid was static and fully opened, and the other where the grid moved randomly (via the triple-random protocol, explained in the next section). Finally, we show that it is possible to check the consistency of the values of C_ε obtained via an adaptation of the Rice theorem to turbulent flows.

II. EXPERIMENTAL SETUP

Experiments were conducted in the Lespinard wind tunnel at LEGI: a large wind tunnel with a measurement section 4 m long and a square cross section of $0.75 \times 0.75\ \mathrm{m}^2$. Turbulence is generated with an active grid made of 16 rotating axes (eight horizontal and eight vertical, with a mesh size $M = 10$ cm) mounted with coplanar square blades (with also a 10 cm side; see Fig. 1). Each axis is driven independently with a step motor whose rotation rate and direction can be changed dynamically. Two different protocols were tested: one where the blades move randomly and one where they remain static. For the random mode (hereafter referred as active grid or AG), the motors were driven with random rotation rates and directions, which were changed randomly in time (the velocity was varied between 1 and 3 Hz, and changes for a lapse were between 1 and 3 s). This mode

FIG. 1. Picture of the active grid used on the present work.

is of widespread use to generate moderate-to-high Re_λ with good HIT conditions and is usually called the triple-random mode. The second protocol employed was the static open mode (referred as open grid or OG), where the grid was completely open (thus minimizing blockage) and static (and therefore generating low values of Re_λ). More details on the active grid and the wind tunnel can be found in a previous work [3].

All measurements were made by means of a single hot wire, using a Dantec Dynamics 55P01 hot-wire probe, driven by a Dantec StreamLine constant temperature anemometer (CTA) system. The Pt-W wires were 5 μm in diameter, 3 mm long, with a sensing length of 1.25 mm. Acquisitions were made for 300 s at 25 and 50 kHz (while a low-pass filter was always set at 30 kHz to counteract aliasing). It was checked that for all the data sets where C_ε results are reported we have at least $\kappa\eta = \frac{2\pi}{U} f\eta = 1$ (with U the local mean velocity).

For each operating protocol, two different kinds of measurements were done: streamwise profiles at constant inlet velocity U_∞, and measurements at fixed streamwise positions ($x = 150$ and $x = 300$ cm) and varying U_∞. The range of U_∞ explored is imposed by the inherent instabilities of the wind tunnel at low velocities, and by the fact that at high U_∞ the grid motors do not have enough power to compensate for the drag force of incoming wind, i.e., it impairs the randomness of the active grid protocol and the closing of the open grid.

For AG (the active grid protocol), one streamwise profile at fixed inlet velocity was recorded at $U_\infty = 6.7$ m/s between $x = 45$ cm and $x = 325$ cm. Next, profiles at fixed downstream position were taken at five different values of U_∞ (1.8, 2.6, 3.6, 5.2, and 6.8 m/s).

For OG (the open grid protocol), three streamwise profiles at fixed inlet velocity were recorded on a similar range as for AG ($U_\infty = 8.6$, 11.9, and 17.0 m/s). Likewise, the profiles for the fixed downstream position were taken at five different values of U_∞ (4.4, 7.0, 9.7, 12.2, and 14.7 m/s).

The registered time signals were subsequently converted into the spatial domain via the Taylor hypothesis. To account for bias of this method, a modified Taylor hypothesis that takes into account a local mean velocity of the flow [16] was also checked, giving almost identical results in both cases. Figure 2 shows the velocity fluctuations' power spectral density obtained for the whole range of velocities—and modes—at the downstream position $x = 300$ cm. It can be observed that they all exhibit a power law close to $-5/3$. Nevertheless, at low values of U_∞, the OG has a less clear

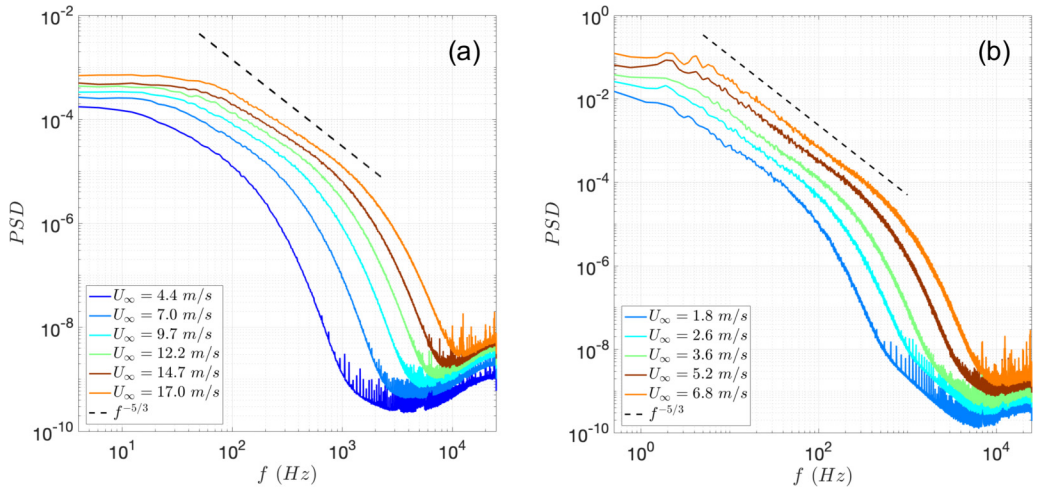

FIG. 2. Power spectral densities of velocity fluctuations obtained at $x = 300$ cm for different values of U_∞ for the open (a) and the active (b) modes. The black dashed line is a $-5/3$ power law.

$-5/3$ exponent, but its shape still remains very similar to other regular static grid spectra previously reported [17].

Large-scale isotropy was quantified with a Cobra probe manufactured by TFI, which is able to compute the three fluctuating velocity components with a resolution of ∼500 Hz. Figure 3 shows the ratios between the three components of the fluctuating velocity vector $\vec{U}' = (u, v, w)$. The active mode exhibits acceptable isotropy conditions, with ratios below 10% for moderate distances away from the grid, i.e., $x > 1$ m. Surprisingly, the isotropy ratios for the open mode are larger (in the order of 30%), and consistent with values reported for fractal grids in the range which comprises nonequilibrium turbulence [18]. Hence, it is seen that reasonable isotropy conditions are found on both modes. However, caution has to be taken when analyzing results coming from the open mode.

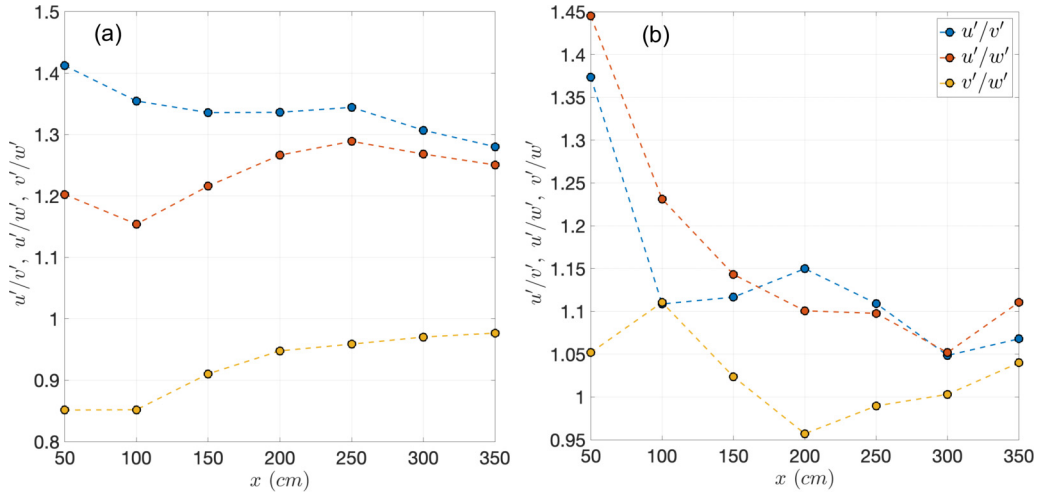

FIG. 3. Ratios between the fluctuating velocity vector $\vec{U}' = (u, v, w)$ components for the open (left) and the active (right) modes. Measurements were taken at $U_\infty = 11.5$ m/s for the first mode and at $U_\infty = 4.9$ m/s for the latter modes.

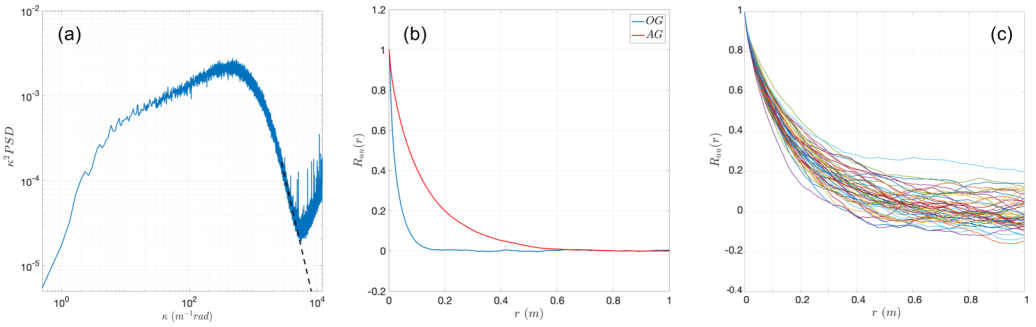

FIG. 4. (a) Estimation of ε via the dissipation spectra; the black dashed line corresponds to the modeled frequencies. (b) Typical autocorrelation functions R_{uu} obtained for both operating modes. (c) Example of the method applied to estimate L for the active mode.

There have been a few studies regarding the turbulence homogeneity in wind or water tunnels employing active grids (see, for instance, [11,19] and the review [2]). Interestingly, Larssen and Devenport ([20]) reported that the flow can be considered as homogeneous if the measuring station is located at two integral length scales from the walls. Another proposed criterion to have homogeneity at the center of the section is to have a mesh size M roughly equal to 10% of the tunnel width [2]. Our measuring station ($75 \times 75\ \mathrm{cm}^2$), and mesh size ($\sim$10 cm) fall within the limits of these criteria, and we will therefore consider our flow to be close to a homogeneous state.

The turbulent dissipation rate ε was estimated via the dissipation spectrum. It was calculated as $\varepsilon = \int 15\nu k_1^2 E_{11} dk_1$ where $E_{11}(k_1)$ is the one-dimensional power spectrum, $k_1 = 2\pi f/U$ is the respective wave number, and f is the Fourier frequency in Hz. The latter involves assuming local, small-scale isotropy and applying the Taylor hypothesis. The noise at high frequencies has been removed and modeled as a power law, fitted for each time signal [Fig. 4(a)]. The Taylor microscale has been obtained from ε as $\lambda = \sqrt{15\nu\langle u^2\rangle/\varepsilon}$.

The integral length scale L was estimated via the streamwise velocity autocorrelation function R_{uu} [Fig. 4(b)]. For OG, it was estimated as $L = \int_0^{r_0} R_{uu} dr$, with r_0 being the smallest value at which $R_{uu} = 0$, and r estimated again via the Taylor hypothesis.

The estimation of L for the AG is more difficult, as the autocorrelation function has the pitfall of not always crossing zero. Thus, it was estimated using a method proposed by Puga and LaRue [13], which consists of dividing the velocity signal into small, not-converged segments, that present a typical dispersion δ in R_{uu} [Fig. 4(c)]. Therefore, L can be computed as $L = \int_0^{r_\delta} R_{uu} dr$, where now r_δ is the smallest value for which $R_{uu} = \delta$. This method, however, presents some ambiguity regarding the absolute value of L, as it strongly depends on the length of the segments chosen to estimate δ. It can be appreciated in Fig. 4 that our choice of small segments yielded large values of δ. This choice reduces the dispersion of L between data sets, but it also reduces the value of L. We have examined for biases with respect to this decision, and it was found that different averages present the same trends.

The previous discussions show that both C_ε and L were estimated without assuming any K41 scalings. Thus, it is possible to compute $C_\varepsilon = \varepsilon L/u'^3$ without any assumptions except for the presence of local homogeneity, which would allow a cascade to operate without interference of one-point flow statistics gradients. The range of turbulence parameters obtained for each operating protocol is shown in Table I. Considering that we have ensured that all our turbulent quantities have reached statistical convergence (as stated, signals were acquired for 300 s), the main error on these parameters comes from the measurement of U_∞ during the calibration of the hot wire (and the subsequent use of the Taylor hypothesis) and from the temperature oscillations (that influence ν). We estimate those errors are roughly ± 0.2 m/s for U_∞, and $\pm 0.5\,^\circ$C (due to possible temperature fluctuations between different calibrations).

TABLE I. Typical turbulence parameter ranges for the open (OG) and active (AG) modes: inlet velocity U_∞, turbulence intensity $u'/\langle u\rangle$, Reynolds number based on the Taylor microscale Re_λ, Taylor microscale λ, Kolmogorov length scale $\eta = (\nu^3/\varepsilon)^{1/4}$, and streamwise integral lengthscale L.

Parameter	OG	AG
U_∞ (m/s)	4.4–17.0	1.8–6.8
$u'/\langle u\rangle$ (%)	2.0–10.0	12.5–45.0
Re_λ	50–200	200–950
λ (mm)	3.0–8.0	7.0–14.0
η (μm)	100–400	100-500
L (cm)	1.0–3.0	5.0–13.0

III. RESULTS

A. Active grid mode

In this section we present results for the grid operated in the active, triple-random, mode. Figure 5 shows different turbulence parameters obtained for the measured streamwise profiles. No peak was observed for the turbulence intensity, including previous measurements done at distance much closer to the grid ($x \sim 10$ cm, not shown here). It can be observed that turbulence intensity has a considerable magnitude, and therefore the Taylor hypothesis should be used with care. Hence, we will only show results in the following for $x > 130$ cm, where the turbulence intensity remains below 25%, similar to results reported in other works [8]. However, the validity of this approach (using the Taylor hypothesis under these conditions) remains an open question and the validity of the use of this hypothesis on active-grid-generated turbulence should be addressed in detail in future works.

From the figures, it can be seen that, first, the magnitude of Re_λ is considerable, and it significantly changes during the downstream evolution of the flow, the latter being an important requirement to disentangle standard from nonequilibrium energy cascade scalings. Second, the length scale L estimated via the method detailed in the previous section is smooth and slightly decreases with x (a surprising result, but similar trends for L have been reported by Thormann and Meneveau for fractal active grids at large x/M [12]). Finally, all parameters from Fig. 5 are quite sensitive to U_∞, even the turbulence intensity (that usually remains constant at fixed x for static grids) and λ and η (not shown in the figure). This phenomenon was also reported in a previous work [11].

The properties of the energy cascade were studied for $x > 1.3$ m (for the reasons previously explained). Figure 6(a) shows C_ε vs Re_λ. There, it can be observed that for all conditions studied C_ε

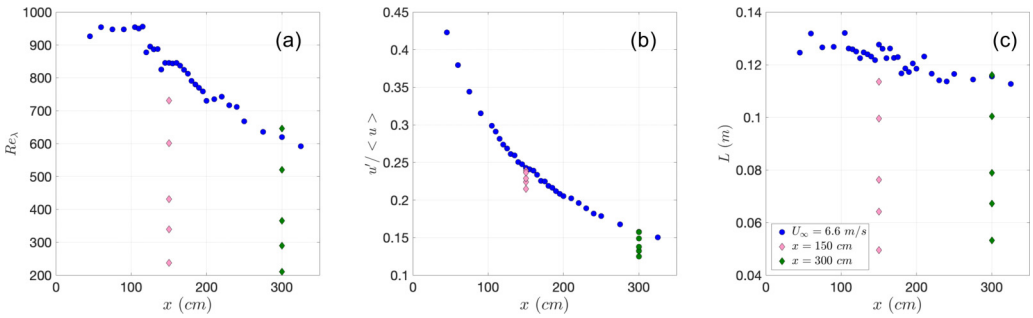

FIG. 5. Streamwise evolution of Re_λ (a), turbulence intensity (b), and integral length scale L (c) for all results obtained for the active mode (AG).

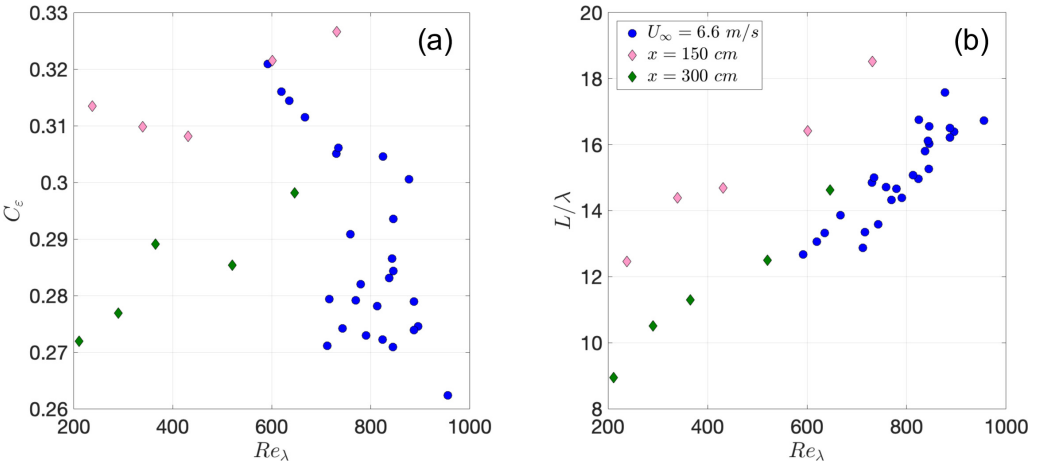

FIG. 6. (a) Plot of C_ε vs Re_λ. (b) L/λ vs Re_λ. Results correspond to all data sets obtained for the active mode.

remains constant: $C_\varepsilon \sim 0.30 \pm 0.03$. This is consistent with standard dissipation scalings and with the relation $L/\lambda \sim C_\varepsilon \mathrm{Re}_\lambda$, that also matches our data [Fig. 6(b)]. The robustness of this outcome validates the use of the Taylor hypothesis in this study and the assumption that the turbulent flow is approximately close to HIT conditions.

Our results, however, differ from those from Puga and LaRue [13] in two ways. First, we do not observe any variation of C_ε with Re_λ (while in the cited work the correlation $C_\varepsilon = 2e^{-0.0108\mathrm{Re}_\lambda} + 0.647$ is proposed). Second, we find smaller values of C_ε. The discrepancy in the magnitudes of C_ε can be attributed to the underestimation of L, as previously detailed. Thus, an alternative method that allows one to check the validity and consistency of the values is required. This will be covered in Sec. III C.

B. Open grid mode

The results for the grid operated in open static mode (OG) are presented below. This case presents important differences with respect to the AG results: for instance, lower values of Re_λ [Fig. 7(a)] and L and much lower values of turbulence intensity. Interestingly, and contrary to the AG, a peak in the downstream evolution of the intensity of the turbulence intensity was captured.

Previous works by Mazellier and Vassilicos [21] and refinements by Gomes-Fernandes and collaborators [22] (for both regular and fractal grids) proposed that the location of turbulence intensity peak could be obtained via the wake interaction length $x_\star$. This model assumes that the maximum of turbulence intensity is a consequence of the interaction between plane wakes, and its downstream location can be therefore modeled, for regular grids, as $x_\star \sim M^2/(C_d t)$, with t being the thickness of the bars and C_d their respective drag coefficient. The value of $x_\star$ depends only on the geometry of the grid and is independent of U_∞ for either regular or fractal grids at large Reynolds numbers.

Conversely, our results with the OG hint that $x_\star$ is an increasing function of U_∞ [Fig. 7(d)]. This is an important difference from previous results in static grids, as it suggest an alternative turbulence generation mechanism not explained by the interaction between wakes, possibly coming from interactions between laminar boundary layers or laminar shear layers, which grow on the surface of the grid blades pointing streamwise. To disentangle the underlying physics of this phenomenon, a broader range of U_∞ should be explored (not currently possible with the present wind tunnel and current grid) in conjunction with a particle image velocimetry (PIV) study close the grid or in the lee of it.

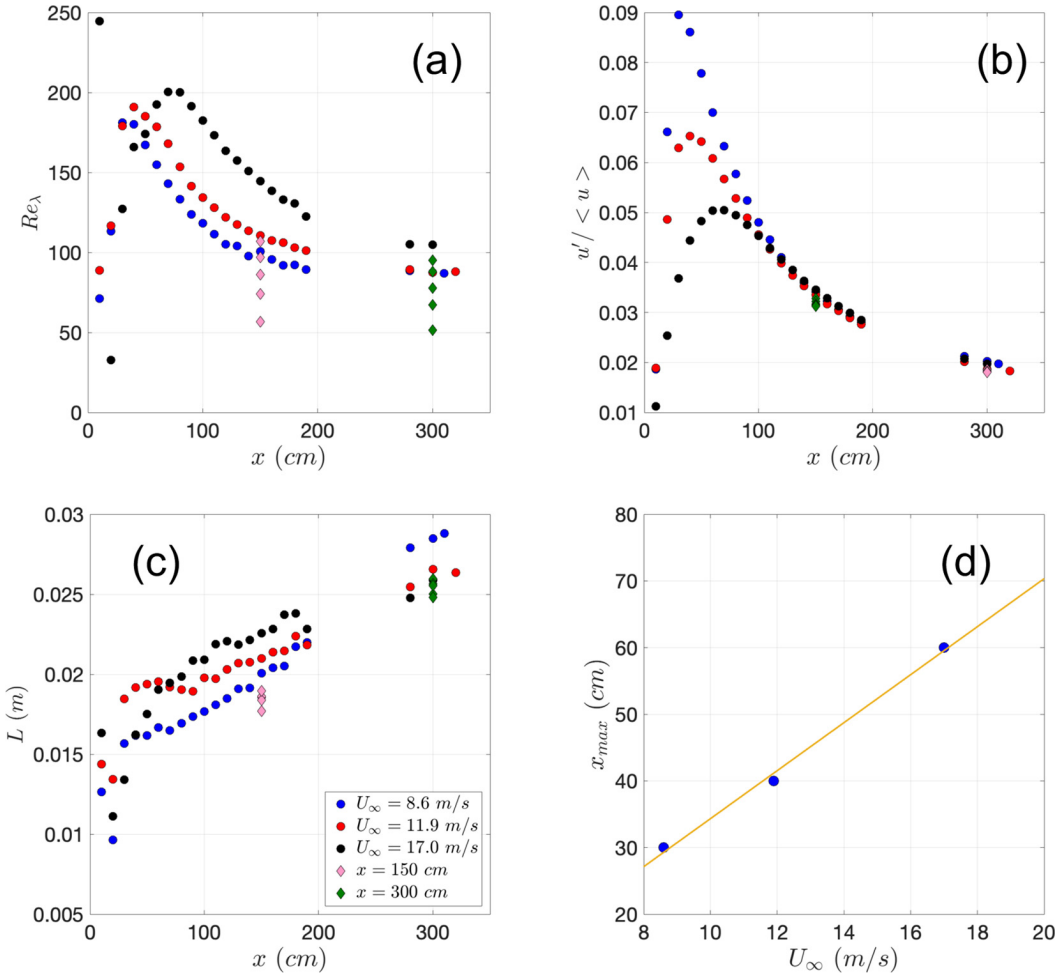

FIG. 7. Streamwise evolution of Re_λ (a), turbulence intensity (b), and integral length scale L (c) for all results obtained for the open mode. (d) Downstream position of the turbulence intensity maximum $x_{\max}$ vs U_∞.

The criterion of Gomes-Fernandez and Vassilicos [22] for the intensity peak is independent of U_∞; it is a consequence of the streamwise scalings of turbulent plane wakes [23,24]. On the other hand, our results exhibit a clear dependence on the inlet velocity, suggesting that the turbulent flow is not entirely (if at all) a result of the interactions between wakes. At our facility, reliable experiments cannot be performed for $U_\infty > 17$ m/s. A broader range of velocities would help to verify how this phenomenon scales with U_∞ and relate it with other mechanisms that may generate turbulent flows, such as laminar and/or turbulent boundary or shear layers interactions. Moreover, it will be very interesting to see how far downstream the peak of turbulence intensity can be shifted (with the consequence that $C_\varepsilon \neq$ constant), and whether or not its downstream location continues to grow with U_∞ or if it has a dependence on the grid or blade parameters. These experiments are of foremost importance, taking into account the research of Mazellier and Vassilicos [25], which cast doubt on the universality of C_ε and its strongly dependence on the flow initial conditions.

As our data for the active mode only exhibit decaying turbulence, we will focus on the same regime for the open mode. We therefore report data only downstream the turbulence intensity peak. Figure 8(a) illustrates that C_ε is a function that varies with $\mathrm{Re}_G/\mathrm{Re}_L$ (and ultimately with Re_λ). Furthermore, at low values of $\mathrm{Re}_G/\mathrm{Re}_L$ it collapses to a straight line, consistent with the high

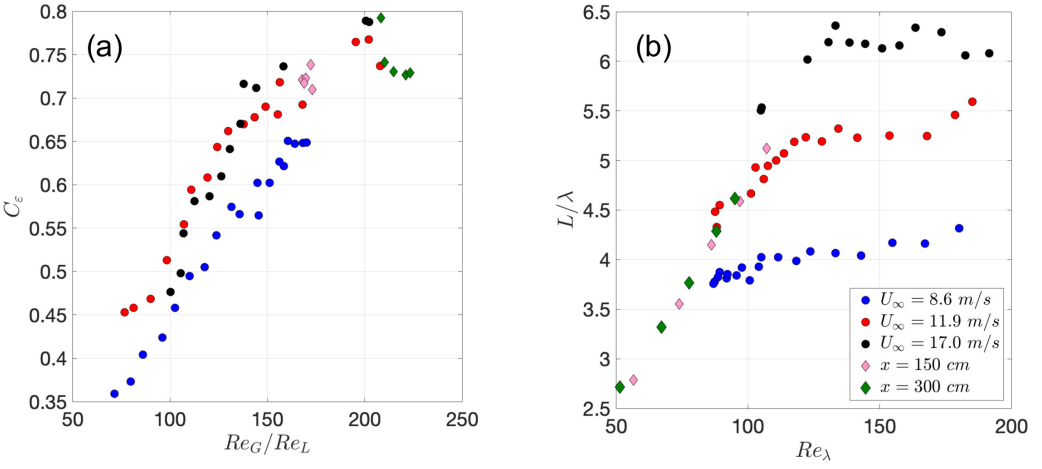

FIG. 8. (a) Plot of C_ε vs $\mathrm{Re}_G/\mathrm{Re}_L$. (b) L/λ vs Re_λ. Results correspond to all data sets obtained for the open mode.

Reynolds nonequilibrium scalings. We also observe that L/λ approaches a constant [Fig. 8(b), the constant having a trend consistent with $\sqrt{\mathrm{Re}_G}$] at large Re_λ (i.e., low $\mathrm{Re}_G/\mathrm{Re}_L$). On the other hand at large $\mathrm{Re}_G/\mathrm{Re}_L$ we note that C_ε becomes constant with Re_λ, and that $L/\lambda \sim C_\varepsilon \mathrm{Re}_\lambda$, consistent with standard dissipation scalings. These figures, similar to those reported by Valente and Vassilicos [26], provide evidence of the presence of both scalings (in separate regions of the flow), i.e., high Reynolds nonequilibrium scalings close downstream from the kinetic energy peak and standard ones after a transition region downstream. The outstanding fact of this transition (previously observed for fractal and regular static grids [26] and in direct numerical simulations of periodic turbulence [15]) is that it occurs at relatively large values of x (while in standard static grids it happens a few cm from the grid), allowing one to capture both regimes in the same experiment. Moreover, the unfixed position of $x_\star$ implies that the open mode can be used to tailor the crossover downstream position between the two scalings. However, the presence of relatively large anisotropy values on the transition downstream position (visible in Fig. 3) suggests that the latter result may not be conclusive. Despite this, and given that the anisotropy barely changes in magnitude for different streamwise positions, the values of C_ε estimated with the full kinetic energy instead of u' follow a similar trend. Further studies on a larger wind tunnel (or with a grid with smaller M) may help to shed light on this phenomenon.

At present, our data suggests that the active grid, depending on the operating protocol selected, will produce different energy cascades, with important consequences for several applications. For instance, apart from the number of degrees of freedom and scale separation, the nature of the cascade will be related to or affected by the persistence of coherent large-scale structures and the turbulent kinetic energy budget, and these will have consequences in terms of turbulence modeling [14,15]. This reinforces the idea to develop an alternative method that allows one to estimate and validate the values of C_ε here obtained.

C. Estimation of ε via the zero crossings of the streamwise velocity fluctuations

Lieppman [27] noticed that the Rice theorem could be applied to the zero crossings of velocity fluctuations to estimate the Taylor microscale λ in turbulent flows. In particular, he mathematically proved that λ is proportional to the average distance $\bar{l}$ between zero-crossings points: $\bar{l} = B\lambda$. The constant B is also defined as $B = C\pi$, where C is a constant that quantifies the non-Gaussianity of velocity derivatives $(\partial u/\partial x)$, where $C = 1$ for a Gaussian distribution and $C > 1$ for an intermittent turbulent flow.

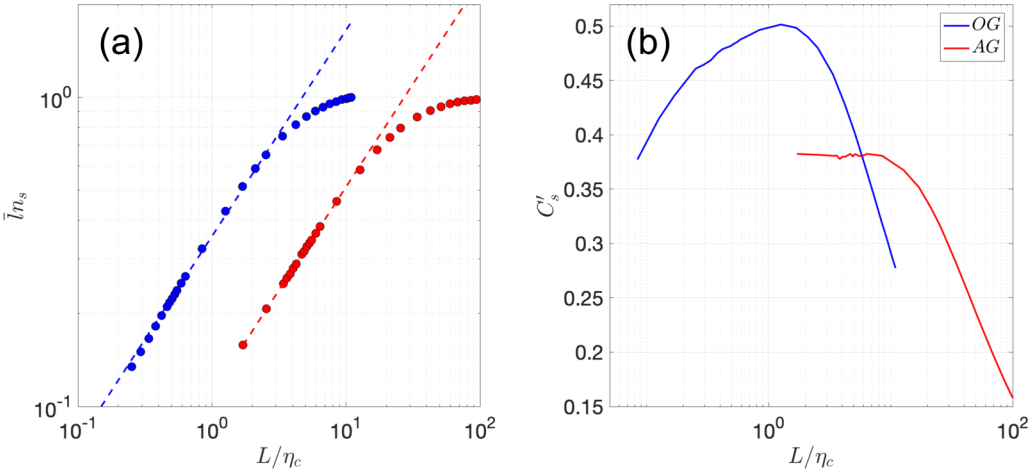

FIG. 9. $\bar{l}n_s$ vs L/η_c (a). The dashed lines are a 2/3 power law. Cs' vs L/η_c (b). Blue lines correspond to the open mode and the red ones to the active one.

However, a theory that allows one to relate C_ε to the number density of zero crossings, n_s, was recently developed by Mazellier and Vassilicos (see [25] for more detailed explanations). This theory relies on the expectation that n_s is a power-law function of L/η_c (as proposed by Sreenivasan and collaborators [28] and by Davila and Vassilicos [29]), n_s being computed after low-pass filtering the turbulent signal with a cutoff frequency $2\pi/\eta_c$ (η_c being the length scale of the filter, not to be confused with the Kolmogorov length scale η). Hence,

$$n_s = \frac{C_s'}{L}(L/\eta_c)^{2/3}, \tag{1}$$

with C_s' a dimensionless constant that characterizes the large scales. The 2/3 exponent is a consequence of the $-5/3$ power-law decay of the power spectral density of the streamwise velocity fluctuations [29]. The constant C_s' also should not be confused with the intermittency constant C (we use the exact same notation and definitions of constants from the seminal work of Mazellier and Vassilicos [25]).

By combining Eq. (1) and the relations $\varepsilon = C_\varepsilon \frac{u'^3}{L}$ and $\lambda = \sqrt{\frac{15\nu u'^2}{\varepsilon}}$, the value of C_ε can be computed as

$$C_\varepsilon = (15B^2)^{3/2}\left(\frac{C_s'}{A^{2/3}}\right)^3, \tag{2}$$

with $A = \eta_*/\eta$. η_* is the value of η_c that corresponds to the intersection of the 2/3 power law and the value $\bar{l}n_s = 1$. At large values of Re_λ, it was found [25] that the latter expression goes as $C_\varepsilon \sim C_s'^3$, which in turn implies that dissipation is controlled by the large scales of the flow. We remark that in the deduction we never required that C_ε be constant (or dependent on $\mathrm{Re}_G/\mathrm{Re}_L$), and therefore Eq. (2) remains valid for any energy cascade (within only approximate HIT conditions, as Mazellier and Vassilicos used the model even for measurements at the center line of a round jet), and in particular for our results for both the open and active modes.

To check the previous prediction, we first checked whether the number density of zero crossings, n_s, followed a 2/3 power law when u was low-pass filtered with different cutoff wave numbers $2\pi/\eta_c$. Figure 9(a) shows that indeed the law was recovered by our data set. As the 2/3 power law has been shown to be a consequence of the $-5/3$ spectrum [30], Fig. 9(a) supports the validity of the results for the OG, that do not clearly follow a power law close to the $-5/3$ law of the velocity

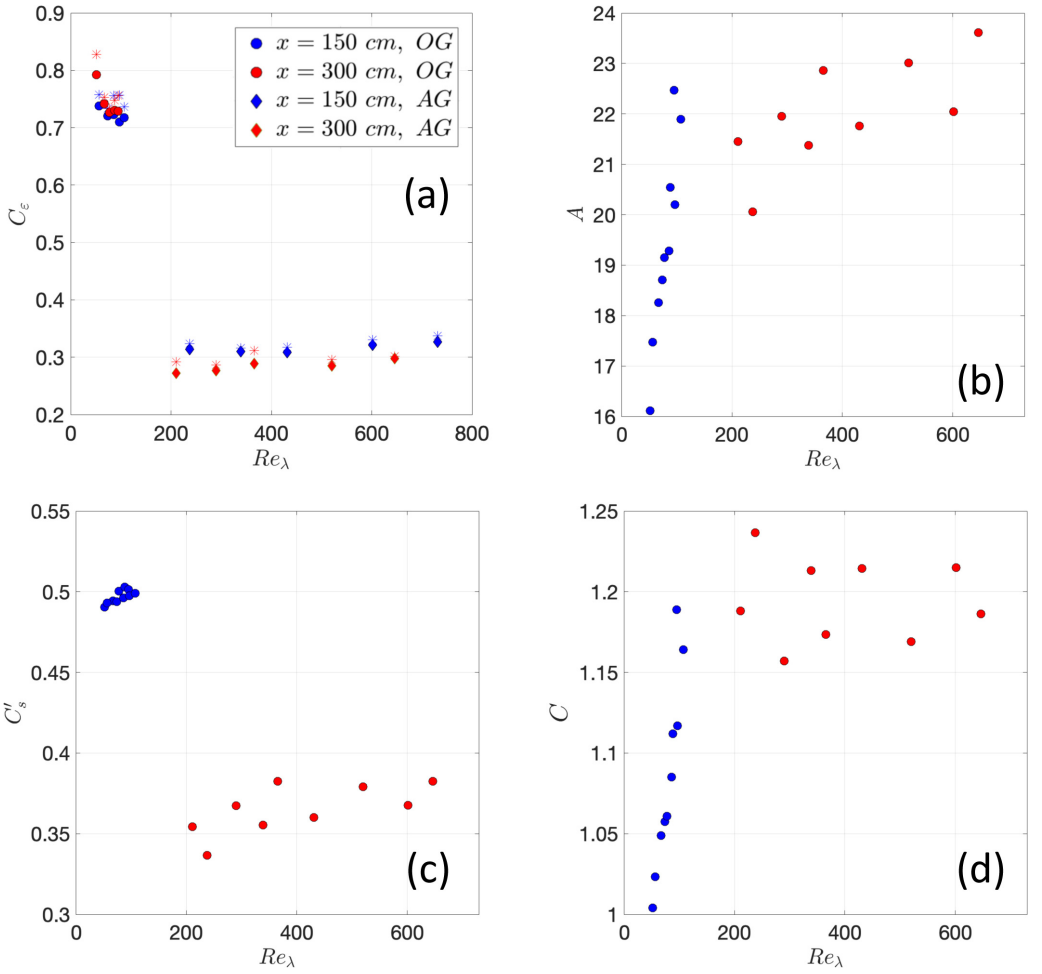

FIG. 10. (a) Comparison of the values $C_\varepsilon^{\text{model}}$ obtained using equation (2) (star symbols) and the experimental ones $C_\varepsilon^{\text{exp}} = \varepsilon L/u'^3$ (filled symbols). Value of A (b), C_s' (c) and the intermittency constant C (d) vs Re_λ for all data sets.

power spectral density (Fig. 2). Furthermore, Fig. 9(b) shows that C_s' is properly defined within the region that follows the power law. The value of C_s' presents a maximum instead of a plateau for the open mode, a consequence of the low values of Re_λ (also observed in previous regular grid measurements at similar values of Re_λ [25]). Therefore, we took the maximum values of C_s' for the open mode.

The results reported here correspond to an antialiasing finite impulse response low-pass filter. We found that the parameter η_* depends on the properties and type of filter used, affecting the values of both A and C_s'. Nevertheless, for all cases, the values of C_ε deduced are very robust [as the dependence on η_* is canceled in Eq. (2)].

Once these requirements were verified, the validity of Eq. (2) could be assessed. The value of C could, in principle, be deduced from the velocity derivatives. However, as the active mode has large values of Re_λ, the convergence of the probability density function of $\partial u/\partial x$ was not completely achieved. Instead, we took this value as $C = \frac{\bar{l}}{\lambda\pi}$.

Figure 10(a) shows streamwise profiles of C_ε for our experimental data and computed from $C_\varepsilon^{\text{exp}} = \varepsilon L/u'^3$ and from Eq. (2) ($C_\varepsilon^{\text{model}}$) for every inflow conditions. The model predictions have

good agreement with all values for the whole range of Re_λ. This remarkable result is an observation of the validity of this model for nonequilibrium turbulence, and, more importantly, it confirms the consistency of the values $C_\varepsilon^{\mathrm{exp}}$ here obtained.

Figures 10(b)–10(d) show the values of A, C_s', and C, respectively. It can be clearly seen that these values strongly depend on the operating mode (OG or AG). The intermittency (indirectly quantified by C) increases with Re_λ and seems to reach a constant value of $C \sim 1.2$ for the active grid mode. As A and B tend toward constant values at large Re_λ, we confirm the prediction that $C_\varepsilon \sim C_s'^3$ for large Re_λ.

IV. CONCLUSIONS

We present a systematic study of the streamwise evolution of active-grid-generated turbulence for two paradigmatic operating modes: a high Re_λ active and random mode and a low Re_λ static one. We found clear evidence that the energy cascade may be strongly influenced by the operating protocol. This outcome has important consequences for active-grid-related research, e.g., the interaction of wind turbines with background turbulence, the formation and development of clusters of inertial particles [31], and other phenomena that rely on the nature of a given energy cascade.

We corroborated previous experimental measurements, which showed that C_ε is constant for active-grid turbulence in the triple-random mode (and therefore consistent with both the Richardson-Kolmogorov cascade and a balanced nonequilibrium energy cascade). On the other hand, we observed that, in a region close downstream the turbulent kinetic energy peak, the open mode followed recently proposed high-Reynolds-number nonequilibrium scalings. Furthermore, this mode seems to be generating a particular type of turbulence (not observed before), which is possibly controlled by the boundary and/or shear layers at the blades of the grid, as the wake interaction length (as defined) is an increasing function of the inlet velocity and is not only dependent on the grid geometry.

Furthermore, we find that the mesh size of the grid is no longer a good estimation of L for any of the tested operating modes. The active mode produces integral length scales on the order of the measurement section (as proposed already in [1]). On the other hand, the open mode has an integral scale of around $1/5$ the mesh size. Remarkably, the same relation between L and M is reported by Mazellier and Vassilicos [21] for fractal-grid-generated nonequilibrium turbulence. Although more studies are needed, this coincidence may point towards a general law relating these two length scales of the flow.

Further studies of intermediate protocols, between the static and random ones, could shed light on underlying mechanics behind the transition from standard to nonequilibrium cascades. Our results seem to agree with the suggestion that nonequilibrium turbulence is related to the presence of large-scale coherent structures [15], as the active mode may destroy them very fast while it could be expected that they are more persistent for the open one. Interestingly, in this work the nonequilibrium energy cascade occurs for the flow at globally lower Re_λ, while for a fixed grid geometry these type of cascade occur close downstream from the grid (and therefore where Re_λ is larger). This is consistent with the findings from [15]: nonequilibrium turbulence does not seem to be a phenomenon that depends uniquely on the Reynolds number of the flow.

Finally, we verified that the model developed by Mazellier and Vassilicos [25] extends to nonequilibrium scalings. This theoretical model, that predicts the value of C_ε from the zero crossings of velocity fluctuations, is a powerful tool to assess the validity of the results obtained when different operating protocols are employed.

ACKNOWLEDGMENTS

We thank Sebastien Torre for his help with installing and operating the traverse system. This work has been partially supported by the LabEx Tec21 (Investissements d'Avenir Grant Agreement No. ANR-11-LABX-0030), and by the ANR Project No. ANR-15-IDEX-02.

[1] H. Makita and K. Sassa, Active turbulence generation in a laboratory wind tunnel, in *Advances in Turbulence 3* (Springer, Berlin, 1991), pp. 497–505.
[2] L. Mydlarski, A turbulent quarter century of active grids: From Makita (1991) to the present, Fluid Dyn. Res. **49**, 061401 (2017).
[3] M. Obligado, T. Teitelbaum, A. Cartellier, P. Mininni, and M. Bourgoin, Preferential concentration of heavy particles in turbulence, J. Turbul. **15**, 293 (2014).
[4] V. N. Prakash, Y. Tagawa, E. Calzavarini, J. Martínez Mercado, F. Toschi, D. Lohse, and C. Sun, How gravity and size affect the acceleration statistics of bubbles in turbulence, New J. Phys. **14**, 105017 (2012).
[5] P. Knebel, A. Kittel, and J. Peinke, Atmospheric wind field conditions generated by active grids, Exp. Fluids **51**, 471 (2011).
[6] R. B. Cal, J. Lebrón, L. Castillo, H. S. Kang, and C. Meneveau, Experimental study of the horizontally averaged flow structure in a model wind-turbine array boundary layer, J. Renewable Sustainable Energy **2**, 013106 (2010).
[7] N. Mordant, Experimental high Reynolds number turbulence with an active grid, Am. J. Phys. **76**, 1092 (2008).
[8] M. Sinhuber, E. Bodenschatz, and G. P. Bewley, Decay of Turbulence at High Reynolds Numbers, Phys. Rev. Lett. **114**, 034501 (2015).
[9] K. P. Griffin, N. J. Wei, E. Bodenschatz, and Gregory P. Bewley, Control of long-range correlations in turbulence, Exp. Fluids **60**, 55 (2019).
[10] L. Mydlarski and Z. Warhaft, On the onset of high-Reynolds-number grid-generated wind tunnel turbulence, J. Fluid Mech. **320**, 331 (1996).
[11] R. J. Hearst and P. Lavoie, The effect of active grid initial conditions on high Reynolds number turbulence, Exp. Fluids **56**, 185 (2015).
[12] A. Thormann and C. Meneveau, Decay of homogeneous, nearly isotropic turbulence behind active fractal grids, Phys. Fluids **26**, 025112 (2014).
[13] A. J. Puga and J. C. LaRue, Normalized dissipation rate in a moderate Taylor Reynolds number flow, J. Fluid Mech. **818**, 184 (2017).
[14] J. C. Vassilicos, Dissipation in turbulent flows, Annu. Rev. Fluid Mech. **47**, 95 (2015).
[15] S. Goto and J. C. Vassilicos, Unsteady turbulence cascades, Phys. Rev. E **94**, 053108 (2016).
[16] J.-F. Pinton and R. Labbé, Correction to the Taylor hypothesis in swirling flows, J. Phys. II **4**, 1461 (1994).
[17] R. A. Antonia, L. Djenidi, and L. Danaila, Collapse of the turbulent dissipative range on Kolmogorov scales, Phys. Fluids **26**, 045105 (2014).
[18] D. Hurst and J. C. Vassilicos, Scalings and decay of fractal-generated turbulence, Phys. Fluids **19**, 035103 (2007).
[19] R. E. G. Poorte and A. Biesheuvel, Experiments on the motion of gas bubbles in turbulence generated by an active grid, J. Fluid Mech. **461**, 127 (2002).
[20] J. V. Larssen and W. J. Devenport, On the generation of large-scale homogeneous turbulence, Exp. Fluids **50**, 1207 (2011).
[21] N. Mazellier and J. C. Vassilicos, Turbulence without Richardson–Kolmogorov cascade, Phys. Fluids **22**, 075101 (2010).
[22] R. Gomes-Fernandes, B. Ganapathisubramani, and J. C. Vassilicos, Particle image velocimetry study of fractal-generated turbulence, J. Fluid Mech. **711**, 306 (2012).
[23] A. A. R. Townsend, *The Structure of Turbulent Shear Flow* (Cambridge University Press, Cambridge, 1980).
[24] W. K. George, The self-preservation of turbulent flows and its relation to initial conditions and coherent structures, in *Advances in Turbulence* (Hemisphere, New York, 1989), p. 3973.
[25] N. Mazellier and J. C. Vassilicos, The turbulence dissipation constant is not universal because of its universal dependence on large-scale flow topology, Phys. Fluids **20**, 015101 (2008).
[26] P. C. Valente and J. C. Vassilicos, Universal Dissipation Scaling for Nonequilibrium Turbulence, Phys. Rev. Lett. **108**, 214503 (2012).
[27] H. W. Liepmann and M. S. Robinson, Counting methods and equipment for mean-value measurements in turbulence research (National Advisory Committee for Aeronautics, Washington, DC, 1953).

[28] K. R. Sreenivasan, A. Prabhu, and R. Narasimha, Zero-crossings in turbulent signals, J. Fluid Mech. **137**, 251 (1983).

[29] J. Davila and J. C. Vassilicos, Richardson's Pair Diffusion and the Stagnation Point Structure of Turbulence, Phys. Rev. Lett. **91**, 144501 (2003).

[30] S. Goto and J. C. Vassilicos, The dissipation rate coefficient of turbulence is not universal and depends on the internal stagnation point structure, Phys. Fluids **21**, 035104 (2009).

[31] R. Monchaux, M. Bourgoin, and A. Cartellier, Analyzing preferential concentration and clustering of inertial particles in turbulence, Int. J. Multiphase Flow **40**, 1 (2012).